Intensity-dependent effects on four-wave mixing based on electromagnetically induced transparency

Gang Wang,[1] Lin Cen,[1] Yi Qu,[2] Yan Xue,[1,3], Jin-Hui Wu,[1,4] and Jin-Yue Gao[1]

[1]*College of Physics, Jilin University, Changchun 130012, China*
[2]*Changchun Institute of Optics, Fine Mechanics and Physics, Chinese Academy of Sciences, Changchun 130033, China*

[3]*xy4610@jlu.edu.cn*

[4]*jhwu@jlu.edu.cn*

Abstract: We extend the study on a four-wave mixing (FWM) scheme of contiuous-wave lasers in a hot rubidium vapor when the probe and coupling fields work in the electromagnetically induced transparency (EIT) regime while the pump and signal fields work in the two-photon Raman regime. Our experimental results show that the generated signal field is well contained in an EIT dip of the incident probe field as a result of efficient FWM. We find, in particular, that an optimal FWM process can only be attained when the coupling and pump fields are well matched in intensity. If the probe intensity is far beyond the EIT condition, however, the nonlinear efficiency of energy transfer from the probe field to the signal field will be greatly reduced.

OCIS codes: (190.4380) Nonlinear optics, four-wave mixing; (270.4180) Multiphoton processes; (020.1670) Coherent optical effects.

References and links

1. S. E. Harris, "Electromagnetically induced transparency," Phys. Today **50**, 36-42 (1997)
2. M. Yan, E. G. Rickey, and Y. F. Zhu, "Observation of absorptive photon switching by quantum interference," Phys. Rev. A **64**, 041801(R) (2001)
3. D. A. Braje, V. Balič, G. Y. Yin, and S. E. Harris, "Low-light-level nonlinear optics with slow light," Phys. Rev. A **68**, 041801(R) (2003)
4. H. Kang and Y. F. Zhu, "Observation of large Kerr nonlinearity at low light intensities," Phys. Rev. Lett. **91**, 093601 (2003)
5. Y. Li and M. Xiao, "Enhancement of nondegenerate four-wave mixing based on electromagnetically induced transparency in rubidium atoms," Opt. Lett. **21**, 1064-1066 (1996)
6. A. J. Merriam, S. J. Sharpe, M. Shverdin, D. Manuszak, G. Y. Yin, and S. E. Harris, "Efficient nonlinear frequency conversion in an all-resonant double-Λ system," Phys. Rev. Lett. **84**, 5308-5311 (2000)
7. D. A. Braje, V. Balić, S. Goda, G. Y. Yin and S. E. Harris, "Frequency mixing using electromagnetically induced transparency in cold atoms," Phys. Rev. Lett. **93**, 183601 (2004)
8. S. A. Babin, S. I. Kablukov, U. Hinze, E. Tiemann, and B. Wellegehausen, "Level-splitting effects in resonant four-wave mixing," Opt. Lett. **26**, 81-83 (2000)
9. H. Kang, G. Hernandez, and Y. F. Zhu, "Resonant four-wave mixing with slow light," Phys. Rev. A **70**, 061804(R) (2004)
10. Y. Wu and X. X. Yang, "Highly efficient four-wave mixing in double-Λ system in ultraslow propagation regime," Phys. Rev. A **70**, 053818 (2004)

#153354 - $15.00 USD Received 23 Aug 2011; revised 13 Sep 2011; accepted 13 Sep 2011; published 18 Oct 2011

11. B. X. Fan, Z. L. Duan, L. Zhou, C. L. Yuan, Z. Y. Ou, and W. P. Zhang, "Generation of a single-photon source via a four-wave mixing process in a cavity," Phys. Rev. A **80**, 063809 (2009)
12. R. M. Camacho, P. K. Vudyasetu, and J. C. Howell, "Four-wave-mixing stopped light in hot atomic rubidium vapour," Nature Photonics **3**, 103-106 (2009)
13. R. C. Pooser, A. M. Marino, V. Boyer, K. M. Jones, and P. D. Lett, "Low-noise amplification of a continuous-variable quantum state," Phys. Rev. Lett. **103**, 010501 (2009)
14. A. M. Marino, R. C. Pooser, V. Boyer, and P. D. Lett, "Tunable delay of Einstein-Podolsky-Rosen entanglement," Nature **457**, 859-862 (2009)
15. Y. W. Lin, W. T. Liao, T. Peters, H. C. Chou, J. S. Wang, H. W. Cho, P. C. Kuan, and I. A. Yu, "Stationary light pulses in cold atomic media and without Bragg gratings," Phys. Rev. Lett. **102**, 213601 (2009)
16. J. Otterbach, R. G. Unanyan, and M. Fleischhauer, "Confining stationary light: Dirac dynamics and Klein tunneling," Phys. Rev. Lett. **102**, 063602 (2009)
17. J. Otterbach, J. Ruseckas, R. G. Unanyan, G. Juzeliunas, M. Fleischhauer, "Effective magnetic fields for stationary light," Phys. Rev. Lett. **104**, 033903 (2010)
18. G. Wang, Y. Xue, J. H. Wu, Z. H. Kang, Y. Jiang, S. S. Liu, and J. Y. Gao, "Efficient frequency conversion induced by quantum constructive interference," Opt. Lett. **35**, 3778-3780 (2010)
19. S. Babin, U. Hinze, E. Tiemann, and B. Wellegehausen, "Continuous resonant four-wave mixing in double-Λ level configurations of Na_2," Opt. Lett. **21**, 1186-1188 (1996)
20. B. L. Lü, W. H. Burkett, and Min Xiao, "Nondegenerate four-wave mixing in a double-Λ system under the influence of coherent population trapping," Opt. Lett. **23**, 804-806 (1998)

1. Introduction

Since electromagnetically induced transparency (EIT) was first demonstrated [1], many interesting phenomena in quantum nonlinear optics have been successfully explored both in theory and in experiment [2, 3, 4]. One important application of EIT is to greatly enhance the four-wave mixing (FWM) process near atomic resonances yet without producing significant absorption. The essence is to create destructive quantum interference in the linear susceptibility but constructive quantum interference in the nonlinear susceptibility by coupling relevant atomic states with a few coherent fields [5]. So far, EIT assisted FWM processes in three-level and four-level atomic systems have been investigated in a variety of laser coupling schemes with the purpose to attain the optimal FWM efficiency. For instance, Harris' group demonstrated the Rabi-frequency matching unique to absorbing nonlinear media [6] and reported an efficient FWM process in cold atoms driven by two counter-propagating laser fields at low light intensity [7]; Babin et al. discussed in particular the level-splitting effect in a resonantly enhanced FWM process in molecular sodium [8]; Zhu's group [9] and Wu et al. [10] reported the resonant FWM with slow light. Quite recently, several applications of resonantly enhanced FWM processes are explored within the topic of single-photon generation [11], high-fidelity light storage [12], quantum state amplification [13], Einstein-Podolsky-Rosen entanglement generation [14] and stationary light manipulation [15, 16, 17].

In Ref. [18], we reported an efficient FWM process of continuous-wave lasers in a hot rubidium vapor with remarkable Doppler broadening. To attain a high FWM efficiency, we adopted a special scheme of light-atom interaction, in which the probe field and the coupling field work in the EIT regime with vanishing detunings while the pump field and the signal field work in the Raman regime with very large detunings. Here we extend this study to examine how the signal intensity is influenced by intensities of the coupling, pump, and probe fields. Our experimental results clearly show that the signal field is efficiently generated in an EIT dip of the probe field and therefore EIT is quite essential for attaining a high FWM efficiency. In addition, there exists a linear relationship between the pump intensity and the coupling intensity for attaining the maximal signal intensity. That is, the pump and coupling fields should be well matched in intensity to pursue an optimal FWM process although they are, respectively, near resonant and far detuned with their driving transitions. Finally, we note that the FWM efficiency will be greatly reduced if the probe intensity goes far beyond the EIT condition.

#153354 - $15.00 USD Received 23 Aug 2011; revised 13 Sep 2011; accepted 13 Sep 2011; published 18 Oct 2011

2. Coherently enhanced four-wave mixing

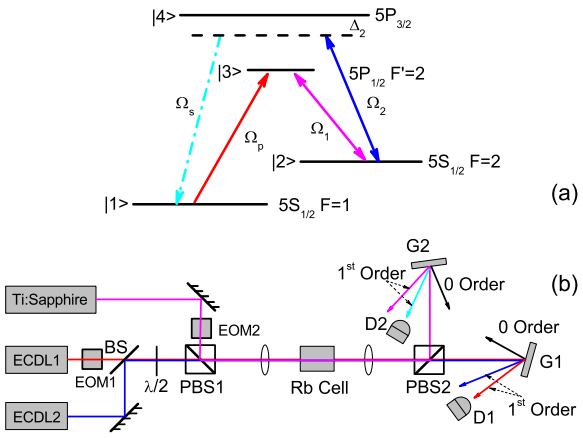

Fig. 1. (a) Diagram of a four-level double-Λ system of ^{87}Rb atoms. The coupling field Ω_1 and the probe field Ω_p are near resonant with their driving transitions $|1\rangle \leftrightarrow |3\rangle$ and $|2\rangle \leftrightarrow |3\rangle$, respectively. The pump field Ω_2 and the signal field Ω_s are far detuned from their driving transitions $|2\rangle \leftrightarrow |4\rangle$ and $|1\rangle \leftrightarrow |4\rangle$, respectively. (b) Diagram of an experimental setup for achieving coherently enhanced four-wave mixing. EOM1 and EOM2: electro-optical modulators; BS: beam splitter; $\lambda/2$: half-wave plate; PBS1 and PBS2: polarization beam splitters; G1 and G2: gratings; D1 and D2: photodiodes.

The diagram of theoretical model is given in Fig. 1(a) while the diagram of experimental setup is shown in Fig. 1(b). A Ti: sapphire ring laser (Coherent 899) is tuned to transition $\left|5S_{1/2},F=2\right\rangle \leftrightarrow \left|5P_{1/2},F'=2\right\rangle$ and acts as the coupling field of Rabi frequency Ω_1; an external cavity diode laser-ECDL1 (DL100) is tuned to transition $\left|5S_{1/2},F=1\right\rangle \leftrightarrow \left|5P_{1/2},F'=2\right\rangle$ and acts as the probe field of Rabi frequency Ω_p; another external cavity diode laser-ECDL2 (DL100) is tuned to transition $\left|5S_{1/2},F=2\right\rangle \leftrightarrow \left|5P_{3/2}\right\rangle$ and acts as the pump field of Rabi frequency Ω_2. In this case, a signal field of Rabi frequency Ω_s may be generated on transition $\left|5S_{1/2},F=1\right\rangle \leftrightarrow \left|5P_{3/2}\right\rangle$ as a result of FWM. The coupling, probe, and pump beams of linear polarizations (either horizontal or vertical) propagate collinearly into a temperature-stabilized vapor cell with the help of a beam splitter (BS), a $\lambda/2$ wave plate, and a polarization beam splitter (PBS1). The vapor cell of ^{87}Rb atoms has a sample length of $L = 3.0$cm and an volume density of $N = 2.2\times10^{11}\text{cm}^{-3}$ at the temperature of $T = 62\ ^oC$. After the vapor cell, the probe field Ω_p and the pump field Ω_2 of horizontal polarizations pass through another polarization beam splitter (PBS2) to arrive in a grating (G1) while the coupling field Ω_1 and the signal field Ω_s of vertical polarizations are reflected by PBS2 to another grating (G2). The grating G1 (G2) with a groove density of 1200 lines/mm can spatially separate the probe (coupling) field Ω_p (Ω_1) of 795 nm and the pump (signal) field Ω_2 (Ω_s) of 780 nm. Photodiodes D1 and D2 are used to monitor intensities of the probe field Ω_p and the signal field Ω_s, respectively.

We first show in Fig. 2 the probe absorption and the signal intensity ($I_s \propto |\Omega_s|^2$) as a function of the probe detuning Δ_p when the coupling field has a vanishing detuning $\Delta_1 = 0.0$MHz. As we can see from the black curves, the signal field is not generated in the absence of the pump field ($\Omega_2 = 0$) and a typical EIT dip centered at $\Delta_p = 0.0$MHz is observed on the Doppler broadened spectrum of probe absorption. On the other hand, the red curves clearly show that

#153354 - $15.00 USD Received 23 Aug 2011; revised 13 Sep 2011; accepted 13 Sep 2011; published 18 Oct 2011

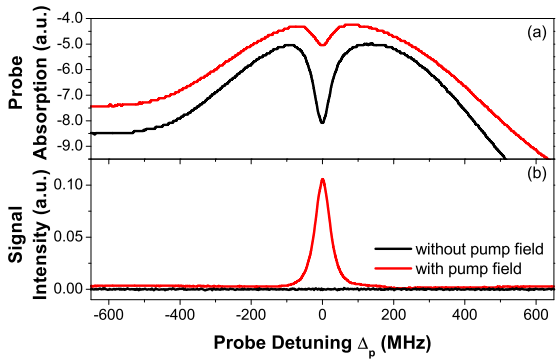

Fig. 2. Probe absorption (a) and signal intensity (b) vs. probe detuning. The black curves are measured in the absence of the pump field while the red curves are attained with $I_2 = 46\text{mW/cm}^2$ and $\Delta_2 = -400\text{MHz}$. Other parameters for the probe and coupling fields are $I_p = 1.2\text{mW/cm}^2$, $I_1 = 62\text{mW/cm}^2$, and $\Delta_1 = 0.0\text{MHz}$.

the signal field is generated inside the EIT dip when the pump filed of detuning $\Delta_2 = -400\text{MHz}$ is turned on ($\Omega_2 \neq 0$). We also find that the EIT dip becomes much shallower due to the nonlinear energy transfer from the probe field to the signal field along the closed pathway $|5S_{1/2}, F = 1\rangle \rightarrow |5P_{1/2}, F' = 2\rangle \rightarrow |5S_{1/2}, F = 2\rangle \rightarrow |5P_{3/2}\rangle \rightarrow |5S_{1/2}, F = 1\rangle$. We have set $\Delta_1 = 0.0\text{MHz}$ for the coupling field while $\Delta_2 = -400\text{MHz}$ for the pump field, which is critical for achieving an optimal FWM process with Doppler broadening. This specific choice has two advantages in improving the FWM efficiency with a remarkable Doppler broadening present: I) to well suppress the energy dissipation in FWM processes due to spontaneous emissions from state $|5P_{1/2}, F' = 2\rangle$ and state $|5P_{3/2}\rangle$; II) to ensure the existence of constructive quantum interference between two competitive FWM processes [18].

Next we show in Fig. 3 the signal intensity as a function of the coupling intensity ($I_1 \propto |\Omega_1|^2$) for four different values of the pump intensity ($I_2 \propto |\Omega_2|^2$). It is clear that, for a given pump intensity, the signal intensity first quickly increases to a maximum and then slowly decreases after this maximum when the coupling field becomes stronger and stronger. Moreover, for a larger (smaller) pump intensity, the maximal signal intensity always corresponds to a larger (smaller) coupling intensity. This means that the maximal signal field can only be attained when the coupling field and the pump field are well matched in intensity. To have a deeper insight, we further plot the pump intensity as a function of the coupling intensity when the maximal signal intensity is attained (see the black curve in Fig. 4). It is clear that there exists a linear relationship between the pump intensity and the coupling intensity for achieving the optimal FWM process. This is a direct evidence for the necessary condition of intensity matching between the pump field and the coupling field. If the intensity matching condition is not fully satisfied, the energy transfer from the probe field to the signal field will be reversed a little so that the signal intensity is reduced to certain extent. In Fig. 4, we also plot the maximal signal intensity as a function of the coupling intensity (see the red curve), where the maximal signal intensity has a largest value when the coupling intensity is 170mW/cm^2 and the pump intensity is 172mW/cm^2.

The experimental results given above are observed in the EIT regime of the probe and coupling fields characterized by $\Omega_p << \Omega_1$ and $\Delta_p = \Delta_1 \approx 0.0$ MHz. Now we begin to examine how the probe intensity I_p influences the signal intensity I_s and thus the FWM efficiency de-

#153354 - $15.00 USD Received 23 Aug 2011; revised 13 Sep 2011; accepted 13 Sep 2011; published 18 Oct 2011

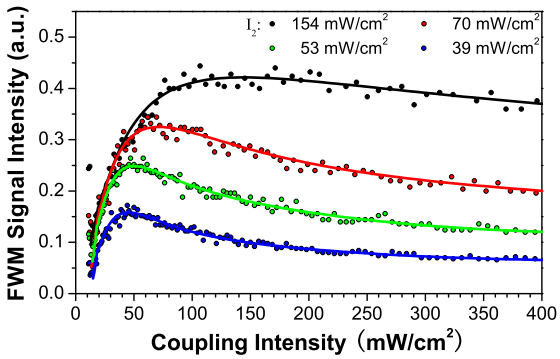

Fig. 3. Signal intensity vs. coupling intensity for four different values of pump intensity. Black, red, green, and blue curves (from top to bottom) correspond to $I_2 = 154\text{mW/cm}^2$, 70mW/cm^2, 53mW/cm^2, and 39mW/cm^2, respectively. The solid curves are guidelines for the experimental data. Other parameters are $I_p = 1.68\text{mW/cm}^2$, $\Delta_p = \Delta_1 = 0.0\text{MHz}$, and $\Delta_2 = -400\text{MHz}$.

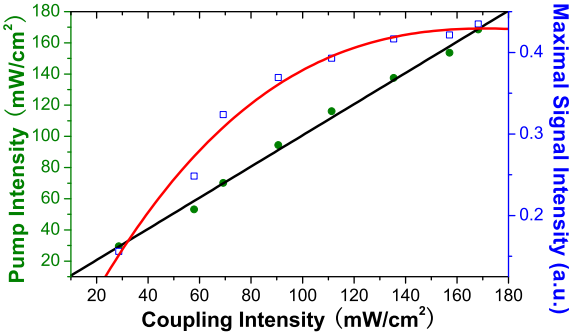

Fig. 4. Pump intensity (filled circles) vs. coupling intensity when the maximal signal intensity (open squares) is attained. The solid curves are guidelines for the experimental data. Other parameters are the same as in Fig. 3.

fined as $\eta = I_s/I_p$. In Fig. 5, the probe intensity is increased from 0.3mW/cm^2 to 10.8mW/cm^2 for the fixed and matched coupling and pump intensities 170 mW/cm^2 and 172 mW/cm^2. We find that the FWM efficiency is almost a constant (about 0.32) and the signal intensity increases linearly with the probe intensity when it is smaller than 1.5mW/cm^2. In this case, the EIT condition $\Omega_p << \Omega_1$ is well satisfied. As the probe intensity goes beyond the condition $\Omega_p << \Omega_1$, however, the FWM efficiency gradually falls down to a very low level (less than 0.08) and the signal intensity reaches its maximal value at $I_p \approx 7.5\text{mW/cm}^2$. Thus we may conclude that EIT plays an essential role in achieving the maximal FWM efficiency and the optimal energy transfer from the probe field to the signal field. Finally, we note that the maximal FWM efficiency could be dramatically improved if a longer Rb vapor cell or a denser atomic sample is employed [18].

#153354 - $15.00 USD Received 23 Aug 2011; revised 13 Sep 2011; accepted 13 Sep 2011; published 18 Oct 2011

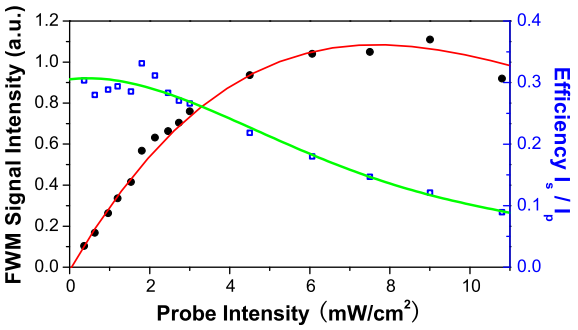

Fig. 5. Signal intensity (filled circles) and FWM efficiency (open squares) as a function of probe intensity. The solid curves are guidelines for the experimental data. Other parameters are $I_1 = 170\text{mW/cm}^2$, $I_2 = 172\text{mW/cm}^2$, $\Delta_p = \Delta_1 = 0.0\text{MHz}$, and $\Delta_2 = -400\text{MHz}$.

Finally, we would like to note that the intensity-dependent effect for FWM have been studied in several previous works [9, 19, 20]. But our experimental results are very different from those in these references as far as the underlying physics and relevant discussions are concerned. First, our experiment is done in a hot Rb vapor under both the EIT condition and the Raman condition. That is, we adopt a special scheme of light-atom interaction, where the probe and coupling fields work in the EIT regime with vanishing detunings while the pump and signal fields work in the Raman regime with large detunings. Second, the large FWM signal in our work greatly benefits from the constructive quantum interference between two concurrent and competitive FWM processes [18] so that the FWM efficiency is greatly enhanced compared with those in refs. [9, 19, 20].

3. Summary

In summary, we have further studied the efficient FWM scheme proposed in ref. [18] by varying intensities of the probe, coupling, and pump fields to control the signal field. We find that the signal field is efficiently generated in an EIT dip of the probe field when the coupling field has a very small detuning while the pump field has a very large detuning. We also find that the maximal signal intensity approximately corresponds to a constant ratio between the coupling intensity and the pump intensity when the probe intensity is fixed. That is, the pump and coupling fields should be well matched in intensity to attain the optimal FWM efficiency. As far as the probe intensity is concerned, however, it should not be too large to go beyond the EIT condition. Otherwise, a very small FWM efficiency will be resulted.

Acknowledgments

This work is supported by the National Natural Science Foundation of China (Grant No. 10904047, 11104111), the National Basic Research Program of China (Grant No. 2011CB921603), and the Basic Research Foundation of Jilin University (Grant No. 200903326).

#153354 - $15.00 USD Received 23 Aug 2011; revised 13 Sep 2011; accepted 13 Sep 2011; published 18 Oct 2011